IOP PUBLISHING JOURNAL OF MICROMECHANICS AND MICROENGINEERING

J. Micromech. Microeng. **22** (2012) 025009 (7pp) doi:10.1088/0960-1317/22/2/025009

Red blood cell sorting with a multi-bed microfabricated filter

Bradley E Layton[1], Bernard Lynch[2], Thomas Peter[3] and Brian Jamieson[2,4]

[1] Department of Applied Computing and Electronics, The University of Montana, 909 South Ave W, Missoula, MT 59802, USA
[2] Detector Systems, NASA Goddard Space Flight Center, Greenbelt, MD 20771, USA
[3] Department of Biomedical Engineering, University of Michigan, 2200 Bonisteel Blvd. Ann Arbor, MI 48109, USA
[4] Scientific and Biomedical Microsystems, 9841 Broken Land Pkwy, Suite 105, Columbia, MD 21046, USA

E-mail: bradley.layton@umontana.edu

Received 24 May 2011, in final form 16 November 2011
Published 13 January 2012
Online at stacks.iop.org/JMM/22/025009

Abstract
A microfabricated fluidic chip for sorting red blood cells (RBCs) by size has been designed, fabricated and tested. The performance of the chip has been compared against a flow cytometer using samples from identical populations of cells, and statistically significant ($p < 0.0005$) differences in the measured cell size distributions were observed. The measurement paradigm reported here differs from previously demonstrated devices such as microfabricated Coulter counters or flow cytometers, in that the analysis is inherently parallel and is thus suitable for high throughput, point-of-care analysis. This study is empirical and semi-quantitative. However, important features of RBC trapping are characterized and indications for improved device design are described.

(Some figures may appear in colour only in the online journal)

Introduction

A complete blood count (CBC) is used to diagnose and manage numerous diseases. Typically a CBC is performed in a laboratory or clinic using a benchtop or stand-alone hematology analyzer, a piece of equipment unsuitable for field medicine and typically inaccessible to smaller or remote clinics (Gulati and Hyun 1994, Shapiro 2004). The results of a CBC can reflect problems such as dehydration, which is manifested by abnormalities in blood cells such as cell production rate, cell life span and cell rate of destruction. The CBC is frequently used to screen infants, institutionalized elderly persons, pregnant women and recent immigrants from economically undeveloped countries if poor nutrition or inadequate iron intake is suspected (Shapiro and Greenfield 1987). Abnormally high or low red blood cell (RBC) count (RBCC) or platelet counts may indicate the presence of many forms of blood diseases or conditions such as stroke (Albers *et al* 2004, Ohira *et al* 2006) or anemia (O'Donnell *et al* 2007). Hence, blood counts are amongst the most commonly performed blood tests in medicine.

Presently, a CBC involves the drawing of several milliliters of blood by a trained phlebotomist, and special processing that may take several hours to a few days. While the practice is routine, the expense involved in traveling to a medical practitioner, and the processing time could potentially be reduced if a smaller, disposable hand-held device similar to a blood glucose sensors, e.g. (Thorsell *et al* 2004) were to be available. For the nearly 4.5 million Americans living with heart disease (Dosh 2004), a condition with an annual estimated cost of over $10 billion (O'Connell and Bristow 1994) and an estimated cost of $400 per test (Blank *et al* 1999), advanced versions of a device such as ours may provide a means for reducing cost and invasiveness, while maintaining reliability.

Since its invention in 1956, the Coulter counter (Coulter 1956, Loos *et al* 1976) has been a standard for cytology. Early innovations in microfabricated counters include several next-generation Coulter-based devices such as the microchip

Coulter particle counter (μCPC) (Bloch*et al* 1978, Larsen *et al* 1997), and a Coulter counter device used in conjunction with a liquid aperture to prevent channel blocking (Nieuwenhuis *et al* 2003). Other recent devices include a polymer microfluidic chip with microchannel bend structures (Blattert *et al* 2004), an electronic detection circuit connected to both a microchannel and microelectrode(s) (Gawad *et al* 2000), a gravity-driven polymeric microfluidic cell sorter (Huh *et al* 2002), a 3D RBC cytogram (Kim *et al* 2003), a micro silicon microelectromechanical system (MEMS) device (Satake *et al* 2002), a computer numerical control-machined Plexiglas-based microchip (Yuen *et al* 2001), a hydrodynamic filtration system (Yamada and Seki 2005), an acoustic particle separation system (Petersson *et al* 2005) and a hybrid mechanical-magnetic system (Seo *et al* 2010).

General particle sorters also include the passing of cells through porous filters that have been fabricated inside of microchannels (Moorthy and Beebe 2003) and the passing of RBC through tapered micropores (Baskurt 1996). The size of the pore required for a RBC to traverse the pore has been modeled and was found to be dependent on RBC surface area, volume and deformability (Abatti 1997). RBC area and volume measurements of individual cells have also been made using parallel microchannels (Gifford *et al* 2003). Cytoskeletal alterations (Gov and Safran 2004, Gov *et al* 2004) and general deformation (Parker and Winlove 1999) will affect the dynamics and therefore deformability of membranes of RBC. Typically however, information on the components of the membrane, and therefore membrane dynamics, has been determined through blood impedance measurements (Zhao *et al* 1993). Additionally, RBC movement through channels or pores has been shown to be affected by cell–cell interactions (Sewchand *et al* 1982, Baskurt *et al* 1997, Bishop *et al* 2001b, King and Hammer 2001a, Briceno *et al* 2004, Pierrat *et al* 2004, Skotheim and Secomb 2007), cell–channel interactions (Sewchand *et al* 1982, King *et al* 2001, Pierrat *et al* 2004, Skotheim and Secomb 2007), media viscosity (Sewchand *et al* 1982, Pierrat *et al* 2004, Skotheim and Secomb 2007) and flow rate (Bishop *et al* 2001a). Flow velocities have also been measured through microchannels or pores using wide/evanescent field illuminations (Gai *et al* 2005) and light-scattering measurements (Magnin 2004). For a comprehensive review of 'blood-on-a-chip' devices, see Buttarello *et al* (1992), Ward (2000), Arroyo *et al* (2005), Toner and Irimia (2005).

Pillar-type filters have been shown by several groups to reliably sort cells by size, and trapezoidal post shapes have been used previously as a method for trapping and measuring the size of individual RBCs (Gifford *et al* 2003). To our knowledge, the present work is the first describing the parallel sorting of large numbers of RBCs into distinct chip areas for potential high throughput analysis of cell size. We name it as 'parallel' sorting, since rather than every cell passing through a single orifice or channel as in Coulter counting, cells travel along multiple paths before arriving in counting bins. Such an approach could be used, for example, to produce a RBC size distribution histogram and derive such CBC parameters as mean cell volume, distribution width and red cell count. Compared to a traditional Coulter counter or its microfabricated counterpart, which perform counting and characterization serially, our design performs a highly parallel sorting function, resulting in cells of different effective diameter being trapped in different regions of the chip. This method would lend itself well to a readout utilizing optical or electrical (e.g. impedance-based) cell counting to determine the number of cells in each size bin. With a dead volume of approximately 2 μL and analysis times on the order of minutes, this paradigm could lend itself to a point-of-care CBC device. To assist field medics, or as a means to providing at-home or small clinical hematology care, we present results for a prototype device for sorting and counting RBCs.

Table 1. Filter bed numbering and dimensions. Note: bed 1 is the furthest downstream.

Bed #	Exit width (μm)	Entrance width (μm)
1	3	5
2	4	6
3	5	7
4	6	8
5	7	9
6	8	10
7	9	11
8	10	12

Methods

Device design

The cell sorter chips (figure 1) consist of eight beds of progressively finer trapping elements, with exit aperture dimensions bracketing the average RBC diameters of 6 to 10 μm (table 1). Each bed consists of 15 rows of squares or trapezoids. We fabricated the square-post filter beds such that the posts were aligned into a square array. On the other hand, we fabricated the trapezoidal-post devices such that rows of posts were staggered. The rationale for fabricating these two geometries was to observe individual cell behavior while simultaneously investigating the efficacy of a device consisting of a series of filter beds with diminishing passage sizes, e.g. (Gifford *et al* 2003). Specifically, trapezoidal features have been found to 'trap' compliant cellular structures that fit into the upstream end, thus arresting them in the tapered feature. In preliminary evaluation of device performance, the trapezoidal elements were found to lead to a greater percentage of trapped RBCs *within* filter beds, while the square elements trapped a greater percentage of trapped RBCs *between* filter beds. Filter beds contain between 350 and 550 filter elements in each row. The exit aperture decreases in 1 μm increments in successive beds, starting at 12 μm and decreasing to 5 μm. A smaller dimension would be necessary for platelet trapping. For the purpose of characterizing flow of individual cells and particles, a transparent Pyrex top was anodically bonded to the silicon filter layer (figures 1 and 2). The Pyrex top was designed with an inlet and an outlet port to which Nanoport^{TM} fittings were attached.

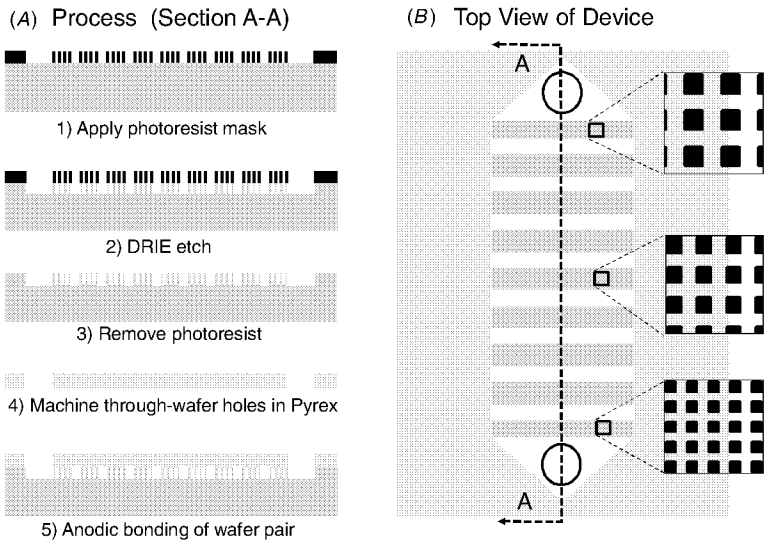

Figure 1. Our wafer fabrication process flow was a three-mask, two-wafer process utilizing silicon DRIE and aligned anodic wafer bonding. (*A*) Cross-sectional view of the device through section A–A. (*B*) Top view schematic of the device. Insets depict relative feature sizes.

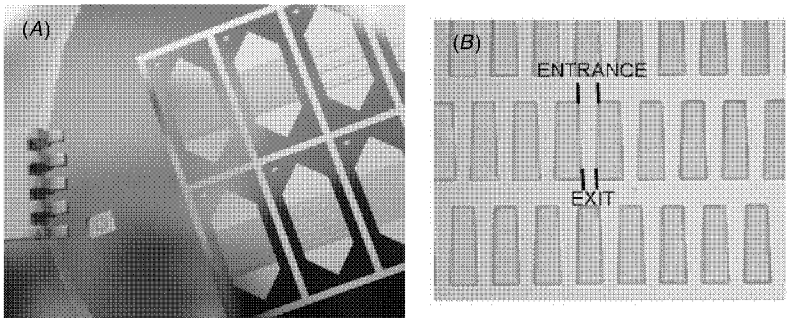

Figure 2. Dimensions of trapezoidal filter elements within each filter bed. A single device is composed eight beds of between 350 and 550 trapping elements.

Basic approach

Sorting cells by size is inherently problematic in that they are typically irregularly shaped, mechanically compliant, variably adherent and susceptible to solution tonicity e.g. (Wandersee *et al* 2005, Nishimura *et al* 2009, Dharmasiri *et al* 2010). In addition (and in contrast to glass spheres) there is no readily available size standard with which to characterize sorting performance. Thus, to answer whether sufficient sizing information can be obtained from a micromechanical lab-on-chip filter to enable the clinically relevant determination of the RBC size distribution, we used fixed cells pre-sorted with an established protocol on a laboratory sorter.

Device fabrication

Microfluidic chips were fabricated with standard semiconductor processes on four-inch silicon substrates. Wafers were patterned with photoresist (Shipley's 1827), and etched in a deep reactive ion etcher (DRIE) utilizing the Bosch process. The following etch parameters were found to yield consistent features and straight (90°) sidewalls: 130 sccm SF_6 and 13 sccm O_2 for 12 s etch; 85 sccm C_4F_8 for 8 s passivation at 600 W. This yielded etch depths of approximately 1 μm per cycle. The etch depth was 8.0 μm for the size cohort trials and 9.0 μm for the whole blood trials. A 4 inch Pyrex 7740 wafer was patterned with 800 μm diameter through-wafer holes, either by wet etching in 49% hydrofluoric acid in water, by weight, utilizing an etch mask consisting of 2 μm of e-beam evaporated gold with platinum seed layer mask or by mechanically drilling with a diamond-tipped drill bit (Precision Microfab, Severna Park, MD). The glass wafer was then anodically bonded to the silicon wafer to form the top of the microfluidic channels and cavities with a bond temperature, 450 °C, a bond pressure of 5 bar and a voltage of 2 kV. The wafer was diced into individual devices to allow for bench-top testing. Scanning electron microscopy images were taken to verify etch depth and feature quality (figure 3). Devices were fabricated at the NASA Goddard Space Flight Center, Greenbelt, MD and subsequently tested at Drexel University and Scientific and Biomedical Microsystems.

Bead sorting

Fabricated chips were connected to a syringe pump with 1/16″ polytetrafluoroethylene (PTFE) tubing and a NanoPort (Upchurch Scientific, Oak Harbor, WA). A second section of

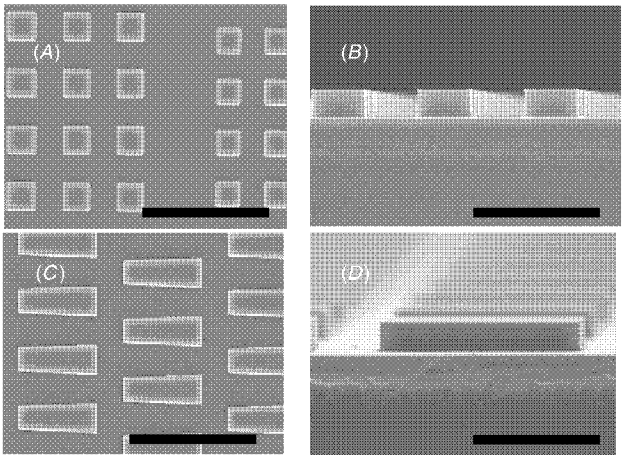

Figure 3. Scanning electron micrograph of silicon filter elements: (*A*) top view and (*B*) side view of a square-post device prior to Pyrex bonding. (*C*) Top view and (*D*) side view of trapezoidal post device prior to bonding. Note that the patterning of (*A*) and (*C*) differ in that the square posts of (*A*) are aligned whereas those in (*C*) are staggered, which forces flow bifurcation and likely increases the chance of a cell ending up in an 'end trapped' state (see results section for images of trapped cells. All scale bars = 20 μm.

1/16″ PTFE tubing was connected to the opposing NanoPort allowing waste to drain into a reservoir. Each chip was flushed with acetone at 0.5 μL s^{-1} for 5 min prior to testing in order to remove organic debris from prior tests. A dilute sample (approximately 1000 beads per mL) of calibrated 4.4, 5.3, 8.3 and 10.0 μm polystyrene micro-beads (Bangs Laboratories, Fishers, IN) suspended in de-ionized water was introduced to the syringe pump, and was allowed to pump through the microfluidic chip for approximately 30 min at a flow rate of 1 μL s^{-1}.

Blood sample standards preparation

The experimental set-up for RBC sorting was similar to that described for bead sorting, except that additional sample preparation was required. For this, whole porcine blood (Galvinell Meat Co., Conowingo, MD) was collected and immediately heparinized (0.9% NaCl, 75 USP heparin/mL). The blood was then sorted into size cohorts within 17 days of collection by flow cytometry using FSC-A light scattering (BD FACS Aria, Maryland Pathogen Research Institute at the University of Maryland). Immediately prior to analysis, the blood was diluted 200:1 in Dulbeccos phosphate buffered saline (PBS) solution (pH 7.4) and fixed (4% gluteraldehyde) for a total of 10 mL of sample solution. We iterated through various dilution ratios, finding empirically that this ratio served the dual purpose of reducing aggregation observed at lower dilutions while simultaneously minimizing the time to complete an individual experiment. Note also, that since our ultimate goal is to develop a device that produces a histogram of cell diameters via an electrical capacitance measurement within each of the beds between the filters that a balance must be struck between a sufficiently large number of cells to produce a chance in capacitance, yet small enough to reduce the number of small cells trapped behind smaller cells. Flow rates were also arrived at empirically: greater flow rates produced excessive back pressure at the Nanoport™ inlet, while lower flow rates caused excessive experimental durations.

Pre-sorting

The purpose of pre-sorting was to allow the introduction of known size distributions into the microchip and thus correlate the pattern of cell trapping with controlled differences in cell sizes. The flow cytometer was calibrated using 4.4, 5.3, 8.3 and 10.0 μm polystyrene micro-beads using bead solutions of concentrations of approximately 1000 000 beads per 10 mL. This calibration was then used to sort cells into 5.3, 8.3 and 10.0 μm populations of 1000 000 cells each. These pre-sorted samples then formed the basis for experimental comparison of microchip sorting ability with that of the flow cytometer.

Blood sorting

Fabricated chips were connected to a syringe pump with 1/16″ PTFE tubing and a NanoPort (Upchurch Scientific, Oak Harbor, WA). A second section of 1/16″ PTFE tubing was connected to the opposing NanoPort allowing waste to drain into a reservoir. Each chip was flushed with acetone at 0.5 μL s^{-1} for 5 min prior to testing. The fixed, diluted and pre-sorted size cohorts of blood cells were pumped through the chip for approximately 30 min at a flow rate of 0.5 μL s^{-1}.

Results

Bead sorting

Basic device functionality and the validity of the experimental set-up were first confirmed by performing several trials utilizing calibrated glass microspheres. As illustrated in figure 4, with a square post design, beads were trapped by the first filter bed with entrance apertures less than the bead diameter. Results were similar for trapezoidal beds, except that beads were trapped at the first bed with exit apertures less than the bead diameter.

RBC sorting

With optical microscopy (400 × magnification), microchips were examined and the cells trapped in each trapezoidal filter region were manually counted and classified. The three basic patterns of cell trapping identified were 'cell wedging', 'end trapping', and 'field trapping'. Wedging (figure 5, arrowheads) was the expected mode of cell trapping, and corresponded to a cell being forced by fluid flow through a passage between trapezoidal blocks and becoming fixed there. End trapping, in contrast, corresponds to a cell that remained immobile on the end of a trapezoid pillar (figure 5, arrow). Finally, field trapping refers to the situation in which cells became trapped in a region free of any pillar features. The relative frequencies of wedge, end and field trapping were 59%, 25% and 16%, respectively. For the purposes of extracting size information, only wedged

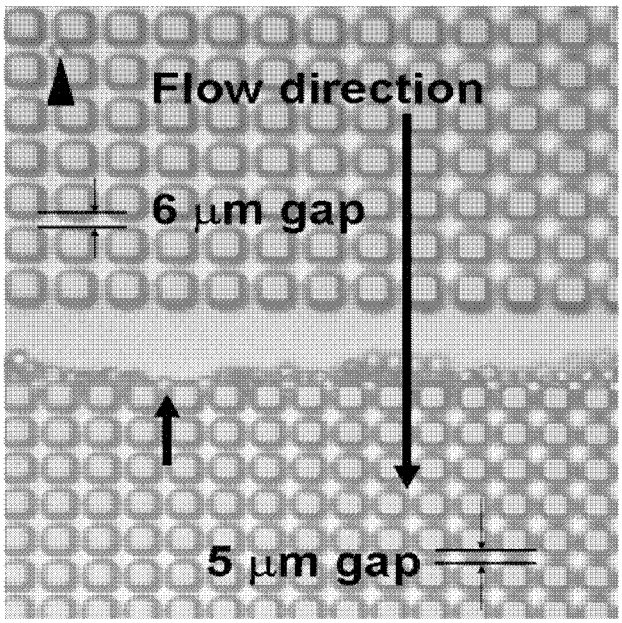

Figure 4. 5.3 μm glass beads passed through 6.0 μm gaps, but were stopped by 5.0 μm gaps (arrow). This process was approximately 99% efficient, as roughly one in one hundred, of the 5.3 μm beads were trapped in the larger filter (arrow head). Note that this image was taken after flow had ceased. Since the tolerance of the test beads is approximately ± 0.1 μm almost no beads made it into the 5 μm filter bed. Note that as discussed above, and as expected, no plastic beads were trapped within the filters of the square post design since they are relatively rigid and gap size is identical within each filter.

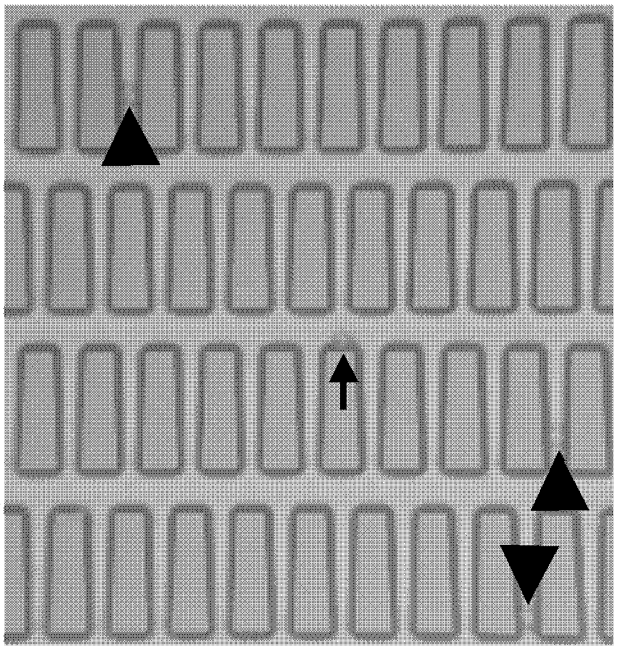

Figure 5. Microphotograph of cell sorter chip showing three RBC's trapped in trapezoidal elements (arrowheads), and a single RBC trapped on a filter element end (arrow). The combination of tapered passages and staggered rows resulted in a greater number of cells trapped within the filters of the trapezoidal design, whereas a greater fraction of trapped cells in the square post design were found between the filter beds.

cells were counted in the cell distribution histogram. Doubly trapped cells and clusters of cells were also ignored for the purposes of analysis; both of these assumptions are discussed in more detail in the discussion section.

Figure 6(*A*) illustrates the distribution of front scattered light intensity from the BD FACS Aria flow cytometer for samples drawn from the 8.3 and 10.0 μm pre-sorted RBC populations. Figure 6(*B*) is the distribution obtained from the chip-based cell sorter using the following method. First we define n, the trapping bed number, as the spacing (in μm) of the exit aperture in which the cell was trapped for $n = 3$ to 9. We can then plot a normalized distribution histogram for the number of cells in each indexed filter region, for both of the two cell populations. While the two distributions have identical modes and medians ($n = 5$) the normalized number per bed, N is

$$N = \frac{\sum_{i=3}^{9} n_i f_i}{\sum_{i=3}^{9} f_i}, \tag{1}$$

where f_i is the relative frequency in the ith bed and n_i is the value of the ith bed, was found to be 4.9 for the smaller (red) cell population and 5.2 for the larger (blue) population. Performing an unpaired two-tailed Student's t-test with unequal variance using MS Excel's TTEST function on the distributions as a whole, resulted in $p < 0.0005$. Thus, the inherent differences in cell size distributions created by pre-sorting can be detected by our device.

Discussion

We present methods for microfabrication and testing of a silicon and Pyrex cell sorting device for sample volumes of 1–10 μL. The data presented here indicate that mechanical filtering with μm-scale patterned filter beds with diminishing dimensions can produce a cell distribution that distinguishes between populations with different size distributions. The mean bed parameter, n, assigned to each region of the filter bed showed a trend, but not equivalence to the mean cell size found within each bed. However, the results support our central claim that the feature size needed to mechanically trap (wedge) a RBC is strongly correlated with cell size and may be used as a proxy for cell size, assuming appropriate calibration. The device was reliable for the size range typical of RBCs and if scaled appropriately may have applications for larger or smaller cells.

The presented method is highly parallel, in contrast to flow cytometry and Coulter counting, both of which analyze a single cell at a time as it moves through an orifice. With a suitable choice of either optical or electronic detection schemes, it should be possible to count cells in a parallel manner. For example, a simple detection scheme would utilize impedance spectroscopy with an array of parallel plate capacitors integrated into the lab-on-a-chip device, with which it would be possible to count cells in each filter region to nearly single-cell accuracy. Another method would be to utilize an on-chip contact image sensor to count cells in each size bin (e.g. filter region). In contrast to wedge trapping, it is not expected

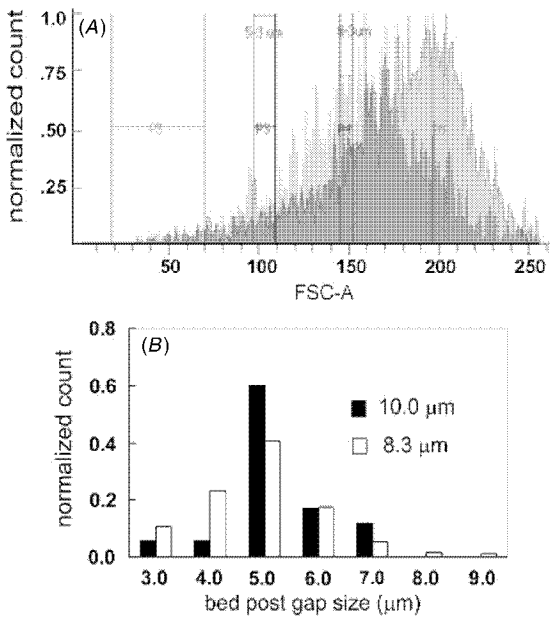

Figure 6. (*A*) RBC size histograms for two different populations of cells, measured with flow cytometry with front scattered optical intensity (FSC-A). Variation in cell size distribution was intentionally introduced by pre-sorting the cells based on size, with an 8.3 μm trigger for the red population and a 10 μm trigger for the blue. (*B*) Cell frequency histogram in different filter regions of the square post design (3 through 9 μm) performed on the same populations of cells as shown in (*A*). Red bars correspond to cell populations pre-sorted with 8.3 μm target cell size and blue correspond to 10 μm gated pre-sorting.

that field trapping or end trapping are governed by cell size, and thus these should ideally be ignored by an automated scheme for cell sizing. Either detection strategy could be arranged to simply ignore end and field trapped cells in the cell distribution, as was done manually for this work.

A potential drawback of our method is that smaller cells introduced into the device in a sample that was not pre-sorted, might potentially become trapped upstream of larger cells. Similar difficulties have been experienced in other recent studies, e.g. (Sim *et al* 2011). This of course would tend to bias the cell count toward larger diameters, since the upstream beds might contain a combination of large and small cells. We thus recommend that pre-sorted are used, as was done in this study, or that sufficiently small samples be used to reduce the chance of this type of interference.

Conclusions

We have successfully designed, fabricated and evaluated a blood cell sorting device capable of sorting a batch of several thousand cells in a volume of 1–10 μL. Efficacy was first demonstrated with a standard set of plastic spheres, and then with a pre-sorted and diluted blood sample. The device has the potential to make at home and remote CBCs less expensive and more reliable.

Acknowledgments

This work was supported by NASA DDF-05-553. The authors would like to acknowledge assistance from Ken Class of the University of Maryland for consultation and use of equipment. We also thank Ms Stephanie Sullivan for preliminary protocol development and Dr Kathleen Allen for researching references. Any opinions, findings and conclusions or recommendations expressed in this material are those of the authors and do not necessarily reflect the views of the National Aeronautics and Space Administration.

References

Abatti P J 1997 Determination of the red blood cell ability to traverse cylindrical pores *IEEE Trans. Biomed. Eng.* **44** 209–12

Albers G W *et al* 2004 Antithrombotic and thrombolytic therapy for ischemic stroke: *7th ACCP Conf. on Antithrombotic and Thrombolytic Therapy Chest* **126** 483S–512

Arroyo M E *et al* 2005 Analytic performance of the PENTRA 80 automated blood cell analyzer for the evaluation of normal and pathologic WBCs *Am. J. Clin. Pathol.* **123** 206–14

Baskurt O K 1996 Deformability of red blood cells from different species studied by resistive pulse shape analysis technique *Biorheology* **33** 169–79

Baskurt O K *et al* 1997 Erythrocyte aggregation tendency and cellular properties in horse, human, and rat: a comparative study *Am. J. Physiol. Heart Circ. Physiol.* **273** H2604–12

Bishop J J *et al* 2001a Erythrocyte margination and sedimentation in skeletal muscle venules *Am. J. Physiol. Heart Circ. Physiol.* **281** H951–8

Bishop J J *et al* 2001b Effects of erythrocyte aggregation and venous network geometry on red blood cell axial migration *Am. J. Physiol. Heart Circ. Physiol.* **281** H939–50

Blank K R *et al* 1999 The utility of serial complete blood count monitoring in patients receiving radiation therapy for localized prostate cancer *Int. J. Radiat. Oncol. Biol. Phys.* **44** 317–21

Blattert C, Jurischka R, Tahhan I, Schoth A, Kerth P and Menz W 2004 Separation of blood in microchannel bends *Proc. IEMBS 04, 26th Annu. Int. Conf. of the IEEE* pp 2627–30

Bloch D *et al* 1978 Flow-cytometric analysis of chicken red blood cells *J. Histochem. Cytochem.* **26** 170–86

Briceno J C *et al* 2004 Radial displacement of red blood cells during hemodilution and the effect on arteriolar oxygen profile *Am. J. Physiol. Heart Circ. Physiol.* **286** H1223–8

Buttarello M *et al* 1992 Evaluation of four automated hematology analyzers. A comparative study of differential counts (imprecision and inaccuracy) *Am. J. Clin. Pathol.* **97** 345–52

Coulter W H 1956 High speed automatic blood cell counter and cell size analyzer *Proc. Natl Electronics Conf.* pp 1034–40

Dharmasiri U *et al* 2010 Microsystems for the capture of low-abundance cells *Annu. Rev. Anal. Chem. (Palo Alto)* ed E S Yeung and R N Zare 3 409–31

Dosh S A 2004 Diagnosis of heart failure in adults *Am. Fam. Physician* **70** 2145–52

Gai H *et al* 2005 Simultaneous measurements of the flow velocities in a microchannel by wide/evanescent field illuminations with particle/single molecules *Lab Chip* **5** 443–9

Gawad S, Henschkel M, Leung-Ki Y, Iuzzolino R, Schild L, Lerch P and Renaud P 2000 Fabrication of a microfluidic cell analyzer in a microchannel using impedance spectroscopy *1st Annu. Int. Conf. on Microtechnologies in Medicine and Biology, 2000* pp 297–301

Gifford S C *et al* 2003 Parallel microchannel-based measurements of individual erythrocyte areas and volumes *Biophys. J.* **84** 623–33

Gov N and Safran S A 2004 Red-blood cell membrane fluctuations and shape controlled by ATP-induced cytoskeletal defects *Biophys. J.* **88** 1859–74
Gov N *et al* 2004 Hydrodynamics of confined membranes *Phys. Rev. E; Stat. Nonlinear Soft Matter. Phys.* **70** 011104
Gulati G L and Hyun B H 1994 The automated CBC. A current perspective *Hematol. Oncol. Clin. North Am.* **8** 593–603
Huh D, Wei H-H, Kripfgans O D, Fowlkes J B, Grotberg J B and Takayama S 2002 Gravity-driven microhydrodynamics-based cell sorter (microHYCS) for rapid, inexpensive, and efficient cell separation and size-profiling *2nd Annu. Int. IEEE-EMB Special Topic Conf. on Microtechnologies in Medicine & Biology* pp 466–9
Kim Y R *et al* 2003 Automated red blood cell differential analysis on a multi-angle light scatter/fluorescence hematology analyzer *Cytometry B; Clin. Cytometry* **56** B 43–54
King M R and Hammer D A 2001a Multiparticle adhesive dynamics: interactions between stably rolling cells *Biophys. J.* **81** 799–813
King M R *et al* 2001 Hydrodynamic collisions suppress fluctuations in the rolling velocities of adhesive blood cells *Langmuir* **17** 4139–43
Larsen U D, Blankenstein G and Branebjerg J 1997 Microchip coulter particle counter *Int. Conf. on Solid State Sensors and Actuators (Chicago, IL)* pp 1319–22
Loos H *et al* 1976 Size distribution, electronic recognition, and counting of human blood monocytes *Blood* **48** 743–53
Magnin O 2004 Blood cell characterization by light scattering *Proc. SPIE* **5461** 1–96
Moorthy J and Beebe D J 2003 *In situ* fabricated porous filters for microsystems *Lab Chip* **3** 62–6
Nieuwenhuis J H, Kohl F, Bastemeijer J and Vellekoop M J 2003 First particle measurements with an integrated Coulter counter based on 2-dimensional aperture control *12th Int. Conf. on TRANSDUCERS, Solid-State Sensors, Actuators and Microsystems, 2003* pp 296–9
Nishimura T *et al* 2009 Label-free continuous cell sorter with specifically adhesive oblique micro-grooves *J. Micromech. Microeng.* **19** 10
O'Connell J B and Bristow M R 1994 Economic impact of heart failure in the United States: time for a different approach *J. Heart Lung Transplant.* **13** S107–12
O'Donnell A *et al* 2007 Age-related changes in adaptation to severe anemia in childhood in developing countries *Proc. Natl Acad. Sci. USA* **104** 9440–4
Ohira T *et al* 2006 Risk factors for ischemic stroke subtypes: the atherosclerosis risk in communities study *Stroke* **37** 2493–8
Parker K H and Winlove C P 1999 The deformation of spherical vesicles with permeable, constant-area membranes: application to the red blood cell *Biophys. J.* **77** 3096–107
Petersson F *et al* 2005 Continuous separation of lipid particles from erythrocytes by means of laminar flow and acoustic standing wave forces *Lab Chip* **5** 20–2
Pierrat S *et al* 2004 Enforced detachment of red blood cells adhering to surfaces: statics and dynamics *Biophys. J.* **87** 2855–69
Satake D *et al* 2002 A sensor for blood cell counter using MEMS technology *Sensors Actuators* B **83** 77–81
Seo H K *et al* 2010 Hybrid cell sorters for on-chip cell separation by hydrodynamics and magnetophoresis *J. Micromech. Microeng.* **20** 095019
Sewchand L S *et al* 1982 Resistance to the Brownian-movement of red-blood-cells on flat horizontal surfaces *Cell Biophys.* **4** 41–6
Shapiro H M 2004 The evolution of cytometers *Cytometry* A **58** 13–20
Shapiro M F and Greenfield S 1987 The complete blood count and leukocyte differential count. An approach to their rational application *Ann. Intern. Med.* **106** 65–74
Sim T S *et al* 2011 Multistage-multiorifice flow fractionation (MS-MOFF): continuous size-based separation of microspheres using multiple series of contraction/expansion microchannels *Lab Chip* **11** 93–9
Skotheim J M and Secomb T W 2007 Red blood cells and other nonspherical capsules in shear flow: oscillatory dynamics and the tank-treading-to-tumbling transition *Phys. Rev. Lett.* **98** 078301
Thorsell A *et al* 2004 Continuous glucose monitoring: a stepping stone in the journey towards a cure for diabetes *J Matern. Fetal Neonatal Med.* **15** 15–25
Toner M and Irimia D 2005 Blood-on-a-chip *Annu. Rev. Biomed. Eng.* **7** 77–103
Wandersee N J *et al* 2005 Erythrocyte adhesion is modified by alterations in cellular tonicity and volume *Br. J. Haematol.* **131** 366–77
Ward P C J 2000 The CBC at the turn of the millennium: an overview *Clin. Chem.* **46** 1215–20
Yamada M and Seki M 2005 Hydrodynamic filtration for on-chip particle concentration and classification utilizing microfluidics *Lab Chip* **5** 1233–9
Yuen P K *et al* 2001 Microchip module for blood sample preparation and nucleic acid amplification reactions *Genome Res.* **11** 405–12
Zhao T X *et al* 1993 Triple-frequency method for measuring blood impedance *Physiol. Meas.* **14** 145–56